

## COMPREHENSIVE MODES OF TELECONNECTIONS BETWEEN SOUTHERN AFRICAN SUMMER RAINFALL AND THE LARGE-SCALE ATMOSPHERIC CIRCULATION

Andreas PHILIPP & Jucundus JACOBETT,  
Würzburg

*Zusammenfassung: Telekonnektions-Modi zwischen Sommerniederschlägen in südlichen Afrika und der großräumigen atmosphärischen Zirkulation.*

Telekonnektionen zwischen interannueller Variabilität des Sommerniederschlags im südhemisphärischen Afrika und dem globalen troposphärischen Druckfeld (GPH) werden mittels bi- und multivariater statistischer Methoden untersucht. Der Kernpunkt der Untersuchung besteht in der Zuordnung einzelner Kopplungen zu verschiedenen grundlegenden Kopplungsmodi, welche die maßgeblichen Beziehungen unter den Fernkopplungszentren beschreiben. Es wird aufgezeigt, dass durch die Verwendung von hochpassgefilterten Zeitreihen eine Optimierung der initialen Korrelationsanalyse zwischen Niederschlag und GPH-Feld erreicht werden kann. Räumliche Zentren mit Maxima der Korrelationen im Druckfeld werden selektiert und in multiplen Regressionsanalysen von redundanter Information bereinigt. Aus den verbleibenden Zeitreihen werden mittels Hauptkomponentenanalyse (PCA) grundlegende Kopplungsmodi ermittelt. Die ersten vier von 11 extrahierten Modi werden anhand ihrer dreidimensionalen räumlichen Muster vorgestellt.

*Summary: Comprehensive modes of teleconnections between southern African summer rainfall and the large-scale atmospheric circulation*

Teleconnections between interannual variability of summer rainfall in southern hemispheric Africa and the global tropospheric geopotential height (GPH) field are examined by means of bi- and multivariate statistical methods. Main objective is the assignment of these relations to different major coupling modes in order to determine the main relations between the various remote coupling centers. It is shown that the use of highpass filtered data is able to optimise initial correlation analyses between rainfall and geopotential height variability. Spatial centers of correlation-peaks in the GPH-field are selected and submitted to multiple regression analyses in order to remove redundant variability. The remaining time series are finally condensed to major coupling modes by means of Principal Component Analysis (PCA). The first four out of 11 modes which have been extracted are briefly presented in terms of their three-dimensional spatial patterns.

*Résumé: Téléconnexions entre les pluies d'été en Afrique méridionale et la circulation atmosphérique à grande échelle.*

Les téléconnexions entre la variabilité interannuelle des pluies d'été en Afrique méridionale et le champ de pression globale troposphérique (GPH) sont étudiées à l'aide de méthodes statistiques bi- et multivariées. L'objectif principal de l'étude est

l'assignation des relations individuelles aux modes fondamentaux de couplage, qui caractérisent les relations décisives entre les centres distants de couplage. Il est démontré que l'analyse de corrélation entre précipitations et GPH peut être optimisée par l'utilisation de séries temporelles filtrées (laissant passer les hautes fréquences). Des centres spatiaux avec des maxima de corrélation dans le champ de pression sont sélectionnés et les informations doubles sont soustraites par des analyses régressives. Les séries temporelles qui restent, donnent les modes de couplage par l'analyse des composants principaux. Les quatre premiers des 11 modes extraits sont montrés avec leur dessin spatial en trois dimensions.

## Introduction

Major amounts of annual rainfall in southern hemispheric Africa are received in the austral summer months, mainly due to the southward penetration of the Intertropical Convergence Zone (ITCZ) and associated circulation systems generating convective rainfall. Beside this simple idea of an regular organized precipitation climatology, influences of varying sea surface temperatures (SST) in the surrounding ocean basins, impacts of the two quasi-permanent subtropical Anticyclones in the south Atlantic and southwestern Indian Oceans, as well as of the midlatitudinal westerlies modulate the spatial distribution and amount of precipitation. The interactions of these influences are also responsible for the pronounced year-to-year variability, with significant impacts on the agricultural economics in wide parts of the subcontinent.

In order to enhance the understanding of this variability, including advances in seasonal prediction approaches (e.g. JURY et al. 1999; LANDMAN et al. 2001), a growing number of studies is dealing with descriptions and analyses of interannual rainfall variability induced by SST and atmospheric circulation dynamics, not only nearby southern Africa but also within remote areas (e.g. the Pacific Ocean). These so-called teleconnections indicate that there are indirectly organized influences on southern African rainfall variability.

Recent studies mainly focus on SST influences of the eastern Pacific (involved into the El Nino / Southern Oscillation (ENSO) phenomenon), of the tropical to southern Atlantic and of the central to southwestern Indian Oceans (CAMBERLIN et al. 2001; RICHARD et al. 2001; NICHOLSON & SELATO 2000; NICHOLSON & KIM 1997; JURY et al. 1999; ROCHA and SIMMONDS 1997a,b; MASON 1995; REASON & MULENGA 1999).

Regarding the southern part of the subcontinent, mainly three influences have been identified in the context of rainfall teleconnections, first to

mention the impact of ENSO signals. In this case a trend to a weakened Walker circulation – associated with El Niño warm events - is detected when rainfall deficits occur in the south. Associated westerly upper tropospheric wind anomalies above the tropical Atlantic Ocean are assumed to play a linking role in that mechanism (JURY 1996; CAMBERLIN et al. 2001). Secondly, trends for negative anomalies of upper tropospheric pressure off the southeast coast of South Africa – representing midlatitude troughs which are known to suppress convection on their westerly rear (TYSON 1986) – are discussed to be involved in this system, too. Thirdly, warm SST anomalies in the Indian Ocean northeast of Madagascar are known to reduce rainfall in the study area, especially examined for southeast Africa (ROCHA & SIMMONDS 1997a,b) and Namibia (SCHINKE & JACOBET 2002). This impact may be independent from ENSO variability.

To learn more about the kind of mechanisms linking the teleconnections onto rainfall variability, it is useful to isolate different types of variability in the geopotential height field being relevant for regional rainfall. Thus major coupling modes between global tropospheric circulation and southern African rainfall will be extracted which are statistically independent from each other, allowing the description of distinctive features of each mode.

Most of the studies mentioned above focus on various rainfall indices representing precipitation variability of local to regional importance, while spatially continuous evaluations of the precipitation field of the whole subcontinent are rare due to a lack of appropriate data. Concerning SST and tropospheric circulation isolated indices are often used, e.g. with respect to ENSO the well known Southern Oscillation Index for the atmospheric part or spatial means of SST in particular areas of the eastern and central Pacific Ocean.

In contrast to the use of isolated indices the present method considers the continuous global tropospheric geopotential height field for teleconnections with rainfall in the continuous area of the whole southern African subcontinent. Only atmospheric pressure is used as predictor variable, however, SST influences are mirrored adequately in the geopotential height field, too.

## **Data sources**

Rainfall data have been received from the CRU05 dataset, representing monthly precipitation amounts for  $0.5^{\circ} \times 0.5^{\circ}$  gridboxes for global land

surface areas. This dataset has been reconstructed based on anomaly signals in the precipitation field as defined by station data (for details see NEW et al., 2000). While data quality in the eastern and southern parts of the present study area is sufficient for analysing interannual rainfall variability, restricted reconstruction skill has to be taken into account for the Congo basin, where local observations are rare and parts of the variability may be artificial due to inadequate extrapolations.

Monthly geopotential height data, describing global atmospheric pressure variability for the 1948-1998 period in a  $2.5^{\circ} \times 2.5^{\circ}$  grid at 7 different levels from near surface (1000hPa) up to the upper troposphere (100hPa), have been extracted from the NCEP/NCAR reanalysis dataset (KALNAY et al. 1996). SST data have been received from Reynolds reconstructed SST dataset (REYNOLDS & SMITH 1995).

### Regional rainfall indices

In order to reduce variability arising from subregional or local scales, all  $0.5^{\circ} \times 0.5^{\circ}$  gridboxes in the domain are condensed to 19 regions according to the maximum among their correlations with 19 temporal variability modes extracted by a rotated Principal Component Analysis (PCA). Figure 1 shows the locations of these resulting regions. For each region a rainfall index is calculated by means of the spatial rainfall mean for each month.

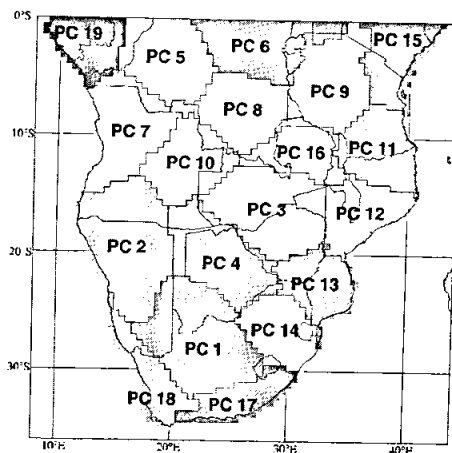


Figure 1. Location of PCA based rainfall regions used for defining regional rainfall indices

This was preferred to the use of statistically independent indices (like the PC scores) in order to keep a spatially continuous field of indices with neighbouring regions including parts of common variability.

### Highpass filtering of time series

On account of considerable shifts in the time series (especially concerning the reanalysis data), which are partly supposed to be natural (e.g. in the mid

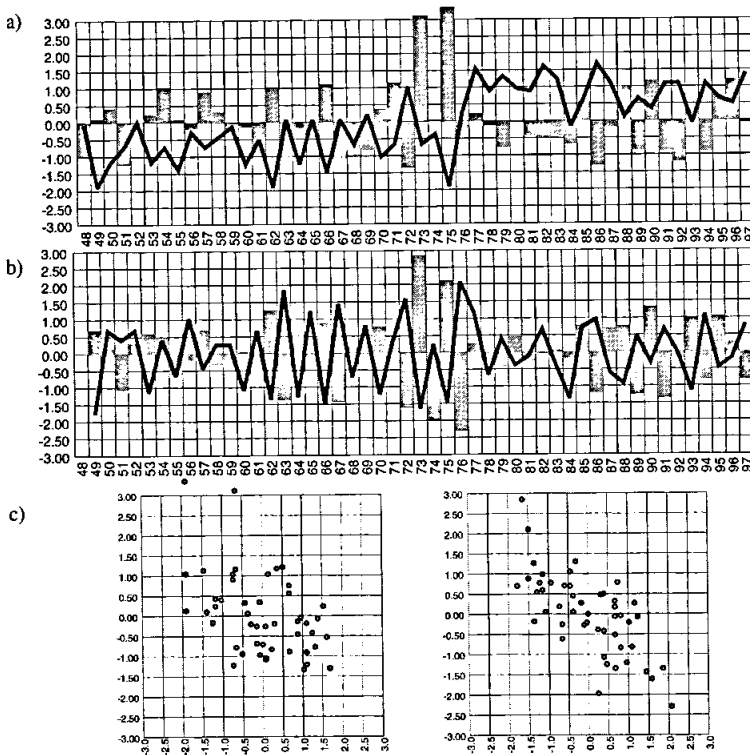


Figure 2. Example time series and scatterplots illustrating the effect of long term variability on correlation coefficients: a) Normalized time series of December-January seasonal means for rainfall index region 1 (bar chart) and 1000 hPa geopotential height at 30°E / 0°S (line plot); b) Same as a) but for highpass filtered (prewhitened) data; c) Scatter plots for normalized raw data of the two time series (left panel) and for prewhitened data (right panel). Correlation coefficients are  $-0.45$  for raw data and  $-0.7$  for prewhitened data.

1970s) but also due to instrumental reasons (e.g. in the 1960s) as pointed out by CAMBERLIN et al. (2001), all time series have been filtered by the so-called prewhitening high pass filter.

A prewhitened time series is simply achieved by calculating the difference between each sample case at time step  $t$  and its predecessor at  $t-1$ . Beside the removal of trends and shifts which may lead to relatively weak and unstable correlations even between strongly covarying time series as stated by Jury (1996), highpass filtering also removes unfavourable temporal autocorrelations as pointed out by BROWN & KATZ (1991). Thus low frequency covariances (e.g. as described by TYSON, 1986) are completely ignored being appropriate for time series with small sample sizes. Figure 2 illustrates the necessity of highpass filtering to point out common high frequency variance which is superimposed by low frequency variations at least in one of the two time series.

## Seasonality

Regarding interannual teleconnections between rainfall in southern Africa and large scale circulation variability, the aspect of seasonality plays a major role for strength and spatial characteristics of these connections. For example, the ENSO influence on rainfall in southern hemispheric Africa is known to be strongest in mid to late summer (December to March) around the Republic of South Africa, whereas in eastern Africa there are strong correlations only in early summer months (October-December). The role of seasonality is pointed out by many authors (CAMBERLIN et al., 2001; NICHOLSON & SELATO, 2000; SCHINKE, 1997; LINDESAY, 1988; KILADIS & DIAZ, 1989; ROPELEWSKI & HALPERT, 1989) being considered by using different seasonal means along the seasonal cycle (e.g. moving three-monthly averages). However, there is an important influence of the seasonal length on the correlations. Due to seemingly unorganized intraseasonal behaviour (ROCHA & SIMMONDS 1997), seasonal means consisting of two or more months are preferred. The fact that most of the teleconnections show strengthening with increasing seasonal length indicates that they are operating on time scales larger than one month.

In the present study seasonality will be considered by using different interval positions along the seasonal cycle as well as different seasonal lengths. Thus, 28 variants of seasonal means are used: months between October and April are combined with seasonal lengths varying from one up to seven months, respectively. To illustrate the changes of correlations by

varying seasonal positions on the one hand and varying seasonal lengths on the other hand, a so-called seasonality diagram has been introduced, showing isolines of correlation coefficients between two time series in a cartesian coordinate system with the temporal center of the seasonal mean on the x-axis, the seasonal length on the y-axis (see Figure 7).

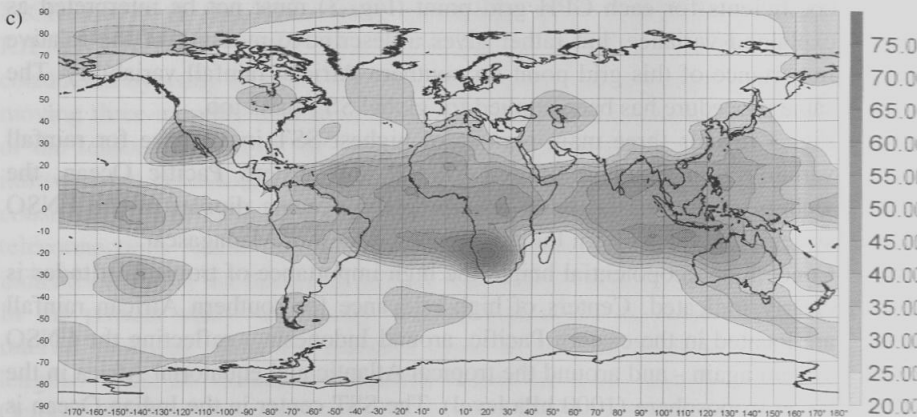
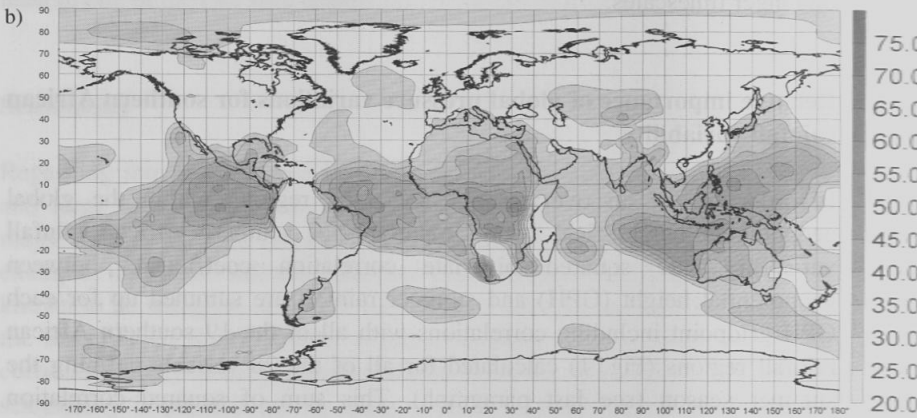
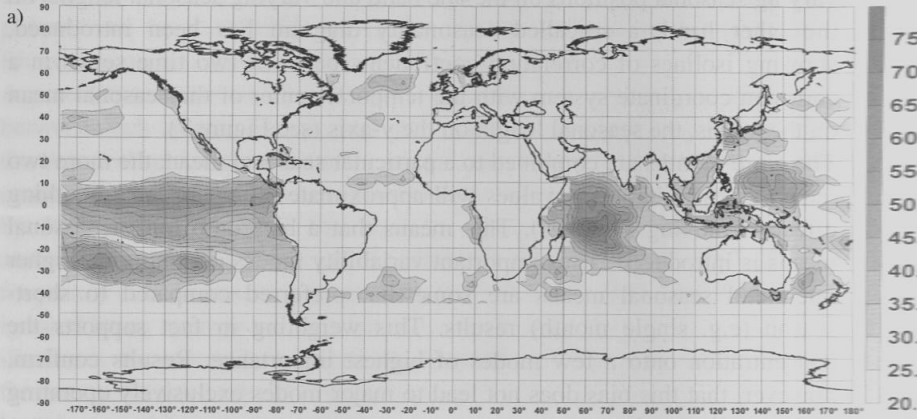
The more months are combined to a particular seasonal mean, the more two temporally neighbouring values will approximate (compare the smoothing effect of moving averages). This means that a bias onto longer seasonal means is introduced. Thus important variability modes operating on higher integrated seasonal means are somewhat preferred compared to short-season (e.g. single month) results. This weighting in fact supports the concentration onto a few modes of highest importance. Results confirm, however, that this bias does not lead to major modes exclusively operating on longer timescales.

### **Relative importance of global pressure variations for southern African rainfall variability**

In order to get an overview of the main regions within the global geopotential height field being important for southern African rainfall variability, the squared bivariate correlation coefficients between geopotential height (GPH) and summer rainfall are summed up for each GPH gridpoint including correlations with all of the 19 southern African rainfall regions (Fig. 1) calculated for all of the 28 variants defining the summer season (see last paragraph). This sum of squared correlation coefficients for each GPH grid point (Fig. 3) must not be interpreted as explained variance, but rather gives a descriptive measure of the relative importance of this grid point for southern African rainfall variability. The same procedure has been applied for global SST data, too.

Fig. 3 reveals three main regions of highest SST importance for rainfall variability in Southern Africa: central and eastern Pacific Ocean, the vicinity of Indonesia (both describing the oceanic dipoles of the ENSO system) and the western Indian Ocean northeast of Madagascar.

Concerning geopotential height the high importance of tropical latitudes is clearly indicated. Centers of high relevance for southern African rainfall are located in the eastern Pacific, around Indonesia – reflecting the ENSO system again - and around the tropical Atlantic and equatorial Africa in the lower troposphere (1000 hPa level). The SST center in the Indian Ocean is less reflected but still well developed.





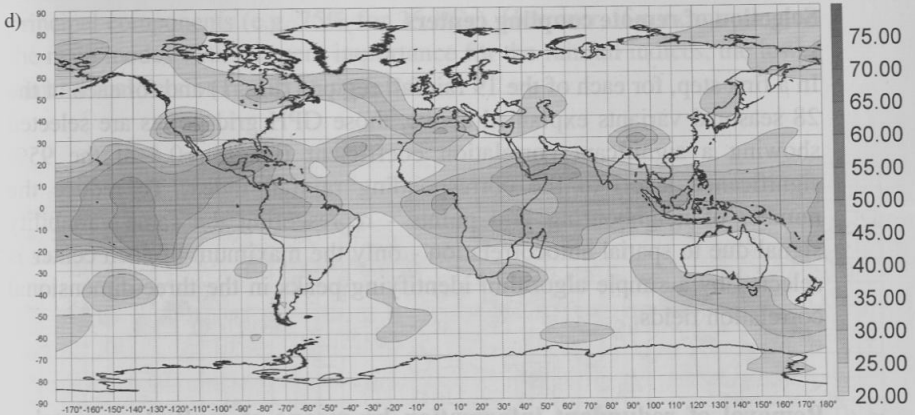


Figure 3. Relative importance of SST and geopotential height variability for southern African rainfall variability, i.e. squared correlation coefficients summed up over all variants of summer seasons (see text) and all southern African rainfall regions. a) SST, b) 1000 hPa, c) 700 hPa and d) 200 hPa geopotential height.

Mid-tropospheric conditions (700 hPa level) partly coincide with the 1000 hPa centers but reveal a new strong center above the Namibian coast, which turned out to be the most important region in the whole global three-dimensional geopotential height field. The upper troposphere - represented by the 200 hPa level - shows a general weakening of relevance, except of a new center above the central Pacific Ocean. This one as well as the eastern Pacific and Indonesian lower tropospheric centers are the primary atmospheric centers of the ENSO system. Beside the above-mentioned tropical centers, further minor centers in the subtropics and midlatitudes (e.g. at the southeast coast of South Africa and south of Australia) are shown in Fig. 3. Their connection to the ENSO system as well as connections between each other are questionable. One major objective of teleconnection analysis therefore arises: splitting up this ensemble of various teleconnection centers into independent coupling modes, accounting for major influences on southern African rainfall variability as a whole. This may indicate some underlying processes of large scale signal transport. The method can be divided into three steps with growing density of information as pointed out below.

## **Selection of remote coupling centers**

In a first step, for each of the 19 rainfall regions (Fig. 1) and for each of the 28 seasonal variants explained above, those GPH grid points are selected showing a significant correlation coefficient (i.e.  $|r| \geq 0.4$  at the 95% significance level) to the corresponding rainfall index. To reduce the number of neighbouring grid points - representing the same variability signal due to spatial autocorrelation - only the maximum of each center is selected by a simple algorithm identifying peaks in the three-dimensional correlation fields.

## **Removal of redundant information by means of multiple regression analysis**

The above selected GPH grid points are used as predictors for multiple regression models with summer rainfall of each region related to each of the summer season variants as predictands, respectively. By means of strict conditions for testing the independence of predictors, only non-redundant information is kept for each regression model, i.e. the partial correlation coefficients are generally strong. Thus, for each rainfall region and each seasonal variant, only a few geopotential height series are remaining, representing different modes in the teleconnections between tropospheric circulation and regional rainfall. The scatter map of predictor locations (Figure 4) includes all predictors of all models revealing some preferred spatial cluster centers which partly coincide with centers of high bivariate importance as presented in Figure 3, e.g. around the Namibian coast, equatorial Africa, off the southeast coast of South Africa and in the Indian Ocean east of Madagascar.

## **Final Principal Component Analysis**

As different summer seasons and different rainfall regions are not independent, some of the predictors still describe quite similar variability. Thus, in a last step, information is further condensed according to the common variability of more than one seasonal variant and more than one rainfall region. This is done by a final rotated principal component analysis with the selected predictor series from the preceding step as input variables. 11 statistically independent modes have been extracted explaining 55% of the original variance. This value would increase with a growing number of

principal components (e.g. 75% for 25 PCs). However, if concentrating on the main modes with frequent importance for the rainfall indices, the lower dimensional version has to be preferred.

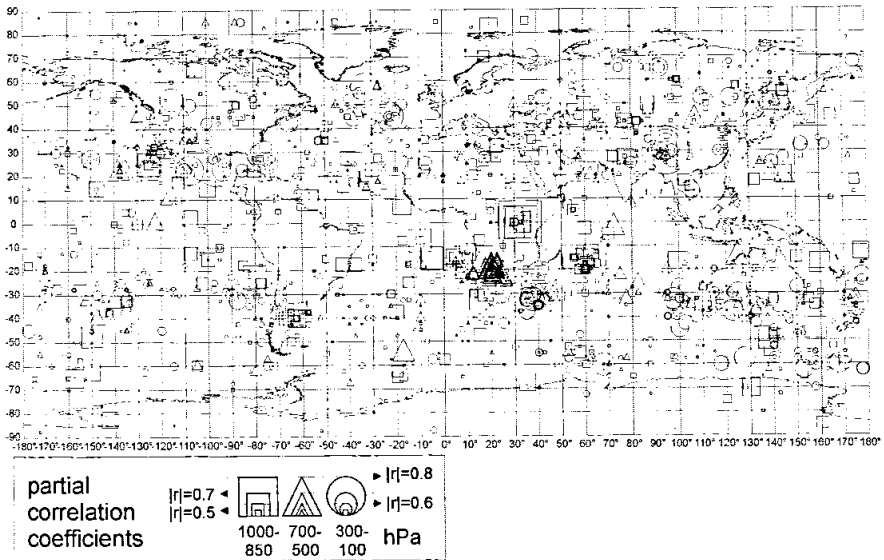


Figure 4. Spatial scatter map of predictor locations as selected by all multiple regression models (geopotential height against summer rainfall) for each southern African rainfall region and each variant of summer season. Symbol size varies with partial correlation coefficients, while the shape of symbols indicates the level of predictors.

### Spatial patterns of resulting modes

In order to determine the teleconnection centers involved in each of the resulting modes, correlations between the PC time coefficients and the prewhitened geopotential height fields have been carried out, thus leading to spatially completed loadings of the PCs, which are referred to as 'loadings' in general henceforth. The patterns represent geopotential height anomalies associated with positive time coefficients of the modes (inverted ones in case of negative time coefficients). All spatial loadings stronger than  $|r|=0.4$  are significant at the 95% significance level.

In order to give a compact overview of the first four of the 11 modes extracted, isocorrelation surfaces have been generated. Figures 5-10 show

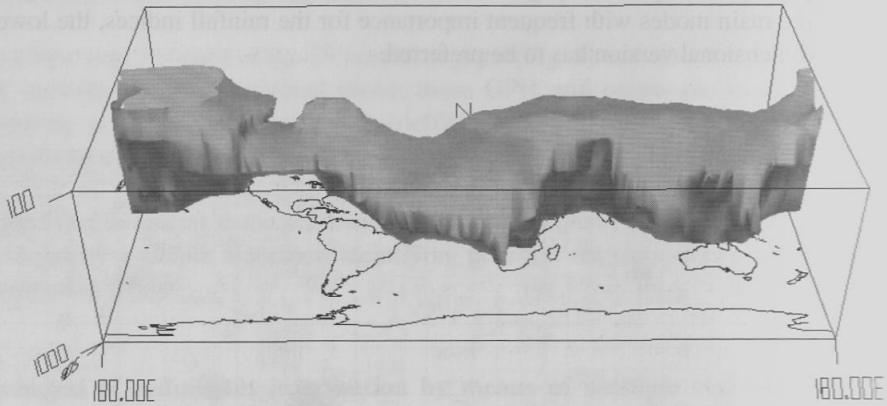


Figure 5. Three-dimensional isocorrelation surface for mode 1 loadings of  $+0.7$  in cylindrical equidistant projection. Height is given in pressure units between the 1000 and 100hPa levels. All grid points inside the surface are correlated stronger than  $+0.7$  with variability of mode 1.

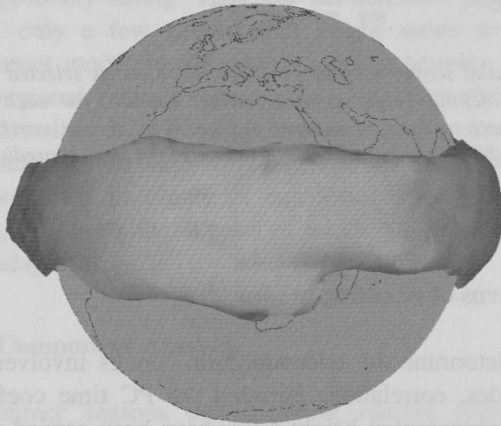


Figure 6. Same as in Figure 5, but in orthographic projection centered on tropical Africa.

surfaces with all their points representing a particular value within the continuous field of loadings, respectively. These surfaces may be regarded as vertical expansions of two dimensional isolines across different pressure levels. Depending on the shape of the resulting volumes, orthographic or cylindrical equidistant projections prove to be appropriate. Figures 5 and 6 depict the domain of high correlations between the geopotential height field and the first mode, including most of the tropical troposphere and much of southern Africa (Figure 6). Some of the above-mentioned centers of high importance for southern African rainfall are integrated within this mode (Figure 5): the low-level centers at Indonesia, tropical Africa and the Atlantic Ocean, the mid-tropospheric center at the Namibian coast, and the high-tropospheric center above the Pacific Ocean. Negative loadings of this domain (not shown) include the Pacific Ocean at low levels. Thus, this mode clearly represents ENSO variability being confirmed by strong correlations between the Southern Oscillation Index (SOI) and the time-coefficients of mode 1, reaching values up to  $r=-0.84$  in the October-March season. Other variants of summer season show weaker correlations, but insignificance only sets in with single-month series in early summer (October and November) according to the seasonality diagram of Fig. 7. Coefficients are generally growing with increasing seasonal length, while there is a pronounced weighting on the second half of the summer period. This may be interpreted as a stronger involvement of the above-mentioned geopotential height centers into the ENSO-system just during late summer.

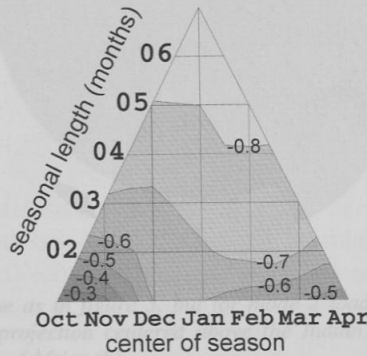
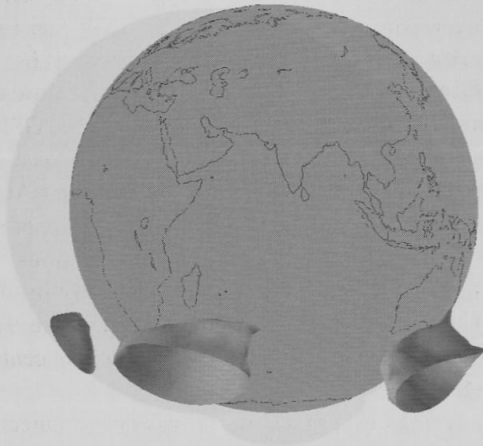


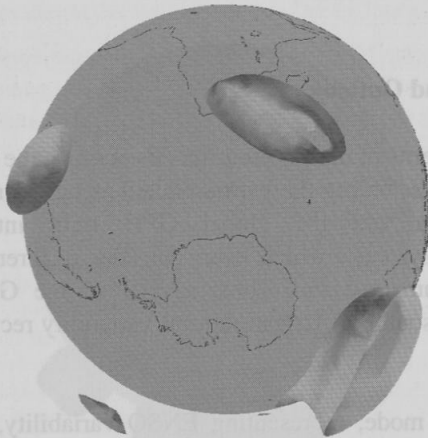
Figure 7. Seasonality of correlations between Southern Oscillation Index (SOI) and the time coefficient of coupling Mode 1. Correlation coefficients vary with seasonal position (x-axis) and seasonal length (y-axis). Contour step is 0.1.

Mode 2 includes four centers of high loadings (Figure 8), all of them at 30° to 40° S with strongest values in the upper troposphere, indicating an extratropical four-wave pattern with centers at 40° E (at the south-east coast of South Africa), 140° E (south of Australia), 120° W (in the south-eastern Pacific Ocean) and 30° W (south-western Atlantic Ocean). The two strongest centers of the wave pattern describe the GPH-teleconnection between the region south of Australia and the east-coast area of southern Africa thus offering an explanation for the link between Australian pressure variations and rainfall in southern Africa in terms of upper wave dynamics. While the first two modes reveal teleconnections inbetween the geopotential height field, mode 3 is represented only by one center in the tropical Indian Ocean north-east of Madagascar (Figure 9). It is restricted to lower tropospheric levels and coincides with the center of high SST importance mentioned before.

Mode 4 shows an extratropical wave pattern connected to pressure conditions of the whole Antarctic region (Figure 10a) which is known as Antarctic Oscillation. The mid-latitude centers are adjusted out of phase to the centers of mode 2 and thus describe a four-wave pattern again – although the Atlantic and the South American centers show some conjunction across the southern Atlantic Ocean. However, the polar center tends to a three-wave pattern with northward extending amplitudes east of Africa, near to Australia and in the eastern Pacific Ocean. Remarkably, wide areas at low levels appear in the tropical eastern Pacific Ocean (Figure 10b) hinting on SST variability being involved in this mode.



a)



b)

*Figure 8. Same as in figure 5, but for mode 2 loadings of +0.4 in orthographic projection centered above the Indian Ocean (a) and centered south of Africa (b).*

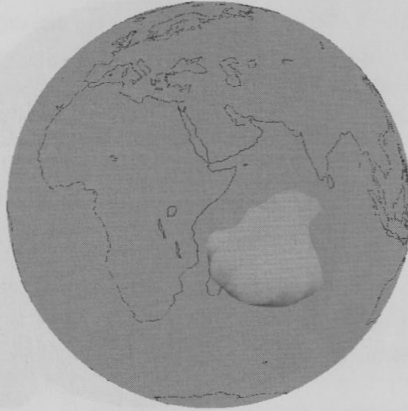


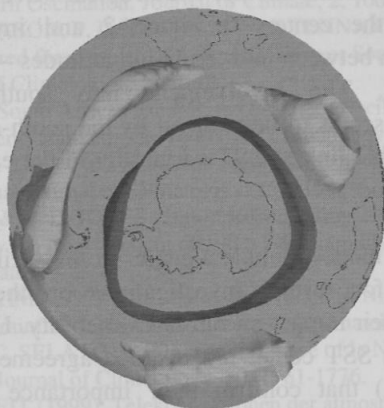
Figure 9. Same as in figure 5, but for mode 3 loadings of +0.6 in orthographic projection centered above the western Indian Ocean.

## Conclusions and Outlook

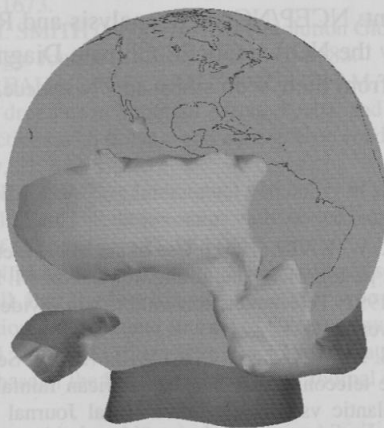
The spatial patterns of the first four modes confirm the presented method to be useful for assembling the various relations between summer rainfall of southern Africa and the global GPH field into different major teleconnection systems, which even consider different operation periods during the summer season. Thus, several of the GPH-centers of high importance for southern African rainfall variability recur in these first four modes:

- The first mode, representing ENSO variability, includes low-level centers at Indonesia, tropical Africa and the Atlantic Ocean, an upper-level center above the central Pacific Ocean and, as a key area for southern African rainfall variations, a mid-tropospheric center at the Namibian coast.
- The second mode represents an extratropical four-wave pattern including teleconnections between upper-level centers above southeast Australia, the eastern Pacific Ocean, the western Atlantic Ocean and the east coast of southern Africa. The latter one may link this mode with rainfall variability due to upper trough configuration.





a)



b)

Figure 10. Same as in figure 5, but for mode 4 loadings of +0.4 (light shaded) and -0.4 (dark shaded) in orthographic projection centered on the South pole (a) and on the tropical eastern Pacific Ocean (b).

- Mode 3 is revealed as a stand-alone low-level center reflecting SST variability in the tropical Indian Ocean.
- Mode 4 represents another extratropical wave pattern, adjusted out of phase to the centers of mode 2 and involved into a seesaw mechanism between mid- and high latitudes – the so-called Antarctic Oscillation. The involvement into southern African rainfall variability seems to be realized by the south-eastern Atlantic center. A remarkable link to SST variability in the eastern Pacific Ocean is indicated, too.

All of these four modes include a center in the vicinity of southern Africa being qualified for further investigations on the underlying physical mechanisms of their impact on rainfall variability. Upper level centers and the Indian Ocean SST center are in good agreement with earlier studies (see Introduction) that confirm their importance for southern African rainfall variations. New aspects on the relations between these centers arise with their actual assembling into major coupling modes which will be subject to a forthcoming paper.

Acknowledgement: NCEP/NCAR Reanalysis and Reynolds SST data have been provided by the NOAA-CIRES Climate Diagnostics Center, Boulder, Colorado, USA, from their Web site at <http://www.cdc.noaa.gov>.

## References

- BROWN, B. G. & R. W. KATZ (1991): Use of statistical methods in the search for teleconnections: past, present, and future. In: Glantz, M. H., R.W.Katz & N. Nicholls (Ed.), 1991: Teleconnections linking worldwide climate anomalies, Cambridge University Press.
- CAMBERLIN, P., S. JANICOT & I. POCCARD (2001): Seasonality and atmospheric dynamics of the teleconnection between African rainfall and tropical sea-surface temperature: Atlantic vs. ENSO. *International Journal of Climatology*, 21, 973-1005.
- JURY, M. R. (1996): Regional rainfall teleconnection patterns associated with summer rainfall over South Africa, Namibia and Zimbabwe. *International Journal of Climatology*, 16, 135-153.
- JURY, M. R., H. M. MULENGA, and S. J. MASON, (1999): Development of statistical long-range models to predict summer climate variability over southern Africa. *Journal of Climate*, 12, 1892-1899.
- JURY, M. R. & S. ENGERT (1999): Teleconnections modulating inter-annual climate variability over northern Namibia. *International Journal of Climatology*, 19, 1459-1475.

- KALNAY E. et al. (1996): The NCEP/NCAR 40-year Reanalysis Project. *Bulletin of the American Meteorological Society* 77, 437-471.
- KILADIS, G. N. & H. F. DIAZ (1989): Global Climatic Anomalies Associated with Extremes in the Southern Oscillation. *Journal of Climate*, 2, 1069-1090.
- LANDMAN, W.A., S.J. MASON, P. D. TYSON & W. J. TENNANT (2001): Retro-active skill of multi-tiered forecasts of summer rainfall over Southern Africa. *International Journal of Climatology*, 21, 1-19.
- LINDESAY, J. A. (1988): South African rainfall, the Southern Oscillation and a southern hemisphere semi-annual cycle. *Journal of Climatology*, 8, 17-30.
- MASON, S. J. (1995): Sea-surface temperature – South African Rainfall Associations, 1910-1989. *International Journal of Climatology*, 15, 119-135.
- NEW, M. G., M. HULME & P. D. JONES (2000): Representing 20th century space-time climate variability. II: Development of 1901-1996 monthly terrestrial climate fields. *Journal of Climate*, 13, 2217-2238.
- NICHOLSON, S. E. & J. KIM (1997): The relationship of the El Niño-Southern Oscillation to African rainfall. *International Journal of Climatology*, 17, 117-135.
- NICHOLSON, S. E. & J. C. SELATO (2000): The influence of la Nina on African rainfall. *International Journal of Climatology*, 20, 1761-1776.
- PHILIPP, A. & J. JACOBET (1999): Telekonnektionen der atmosphärischen Zirkulation des südlichen Afrikas im Südsommer. *Zbl. Geol. Paläont.*, T.1, H. 3-4, 159-178.
- REASON, C. J. C. & H. MULENGA (1999): Relationships between South African rainfall and SST anomalies in the southwest Indian Ocean. *International Journal of Climatology*, 19, 1651-1673.
- REYNOLDS R. W. & T. M. SMITH (1995): A High-Resolution Global Sea Surface Temperature Climatology. *Journal of Climate*, 8, 1571-1583.
- RICHARD Y., FAUCHEREAU N., POCARD I., ROUAULT M. & TRZASKA S. (2000): XXth Century droughts in Southern Africa: Spatial and Temporal Variability, Teleconnections with oceanic and atmospheric conditions. *International Journal of Climatology*, 21, 873-885.
- ROCHA, A. & I. SIMMONDS (1997a) : Interannual variability of south-eastern African summer rainfall. Part I: Relationships with air-sea interaction processes. *International Journal of Climatology*, 17, 235-265.
- ROCHA, A. & I. SIMMONDS (1997b) : Interannual variability of south-eastern African summer rainfall. Part II. Modelling the impact of sea-surface temperatures on rainfall and circulation. *International Journal of Climatology*, 17, 267-290.
- ROPELEWSKI, C. F. & M. S. HALPERT (1989): Precipitation Patterns Associated with the High Index Phase of the Southern Oscillation. *Journal of Climate*, 2, 268-284.
- SCHINKE, H. (1998): Sommerniederschläge in Namibia und ihr Zusammenhang mit der atmosphärischen Zirkulation. *Zbl. Geol. Paläont. Teil I*, 1/2, 147-159.
- SCHINKE, H. & J. JACOBET (2002): Large-scale atmospheric circulation patterns linked to anomalies of Namibian summer rainfall. *Petermanns Geogr. Mitt.*, 146, 2002/3: 28-33
- TYSON, P.D. (1986): *Climatic change and variability in Southern Africa*, Oxford university press, Cape Town.

*Andreas PHILIPP & Jucundus JACOBET*  
*Geographisches Insitut der Universität Würzburg*  
*Am Hubland*  
*D- 97074 Würzburg*